Examining the critical phenomenon of pion parton distribution: Insights from the Moment Problem

Xiaobin Wang,[1,*] Zexin Wu,[1,†] Minghui Ding,[2,‡] and Lei Chang[1,§]

[1] *School of Physics, Nankai University, Tianjin 300071, China*
[2] *Helmholtz-Zentrum Dresden-Rossendorf, Bautzner Landstraße 400, 01328 Dresden, Germany*

A recent study by Wang *et al.*(arXiv:2309.01417) proposed a novel connection between the nature of the parton distribution function (PDF) and the characteristics of its moments. In this study, we apply these findings to analyze the evolution of the pion valence quark PDF, garnering valuable qualitative insights. Firstly, we validate the non-negativity and continuity of the PDF across a wide range of scales, indicating the logical consistency of our chosen evolution scheme. Subsequently, we examine the unimodality of both the PDF and its transformed counterpart, the xPDF, i.e., the parton distribution function multiplied by the momentum fraction. We observe a smooth evolution of the peak position of the xPDF towards the small-x region with increasing scale, while intriguingly, the PDF undergoes a phase of bimodal competition as the energy scale evolves.

I. INTRODUCTION

Throughout history, there has been a great fascination with the intricate structure of particles. One pivotal advancement was Feynman's introduction of partons [1], which postulated that hadrons involved in high-energy collisions could be understood as combinations of numerous point-like partons. Subsequently, Bjorken applied this notion of partons to electron-nucleon deep inelastic scattering processes, elucidating the Bjorken scaling phenomenon observed in the structure function of the proton [2]. This scaling behavior is observed in the asymptotic limit, where the squared transferred momentum of the exchanged virtual photon Q^2 tends to infinity. In this limit, the structure function of the proton demonstrates scaling solely with respect to the light front momentum fraction x, regardless of Q^2. However, the experimentally and theoretically discovered Bjorken scaling violation catalyzed the formulation of the quantum field theory characterized by asymptotic freedom, quantum chromodynamics (QCD). QCD has now become the basis for describing high-energy collision processes, framing the connection between hadrons and partons through the concept of factorization [3]. This framework systematically separates short-range interactions between partons from long-range interactions associated with the color confinement, where one of the physical quantities describing the long-range interactions is the parton distribution function (PDF). It can be seen that the scale dependence phenomenon plays a crucial role in establishing the QCD factorization, and the PDF is scale-dependent.

At one extreme, in the ultra-high energy scale regime characterized by the asymptotic limit ($Q^2 \to \infty$), it has been found that for any given hadron, the first moments of the PDFs, denoting the light-front momentum fraction carried by various partons, exhibit different values. Valence quarks, sea quarks, and gluons exhibit $\langle x \rangle_q = 0$, $\langle x \rangle_s = 3/7$, and $\langle x \rangle_g = 4/7$, respectively [4]. This signifies that in the asymptotic limit, the valence quark PDF is effectively represented as a Dirac delta function centered at $x = 0$. Conversely, in the low energy scale regime, there is a widely discussed current assertion that there exists a hadron scale [5, 6] at which the valence quarks carry all of the light-front momentum of the hadron, with no presence of sea quarks or gluons at this energy scale. Assuming that this assertion holds and taking into account isospin symmetry, the valence quark PDF for the pion is a unimodal distribution, with a single peak positioned at $x = 1/2$ [7, 8]. This stark dichotomy raises a natural inquiry: How do these different manifestations of valence quark PDFs evolve from one configuration to the another?

A comprehensive understanding of the evolutionary path of these PDF profiles requires a full exploration of the underlying dynamics that govern the hadron structure at different energy scales. While the Dokshitzer-Gribov-Lipatov-Altarelli-Parisi(DGLAP) evolution equation is widely recognized for describing PDFs at various scales, in recent years an all-orders evolution scheme has been developed [9, 10]. This innovative approach employs the process-independent (PI) effective charge of QCD to integrate the one-loop DGLAP equation [11]. In contrast to the conventional DGLAP scheme, where the running coupling exhibits infrared divergence, the process-independent effective charge employed in the all-orders evolution scheme is finite at all scales, from the infrared to the ultraviolet, and matches the behavior of the running coupling in the ultraviolet [12]. Notably, empirical validations have demonstrated the effectiveness of this evolution scheme in elucidating both meson and baryon systems [13, 14]. Given the compelling evidence for the all-orders evolution scheme, we opt to employ it herein.

In addition to the novel evolution scheme, an innovative perspective for studying PDFs has emerged: the application of the mathematical Moment Problem [15].

* wangxiaobin@mail.nankai.edu.cn
† wuzexin@mail.nankai.edu.cn
‡ m.ding@hzdr.de
§ leichang@nankai.edu.cn

Typically, theoretical methods [16] or Lattice QCD simulation [17–19] yield low-order moments, while the precise shape of the PDF remains elusive. Using the moment problem framework to analyze these moments provides a very effective way for extracting information regarding the PDF. Notably, this method furnishes insights into the location of the PDF's peaks, thereby facilitating the determination of the modal characteristics of the PDF, especially whether it exhibits a single peak, double peaks, or multiple peaks. This paper focuses on elucidating these modal features. Central to our study is to explore the evolutionary path of the pion valence quark PDF, i.e., the evolution from a single-peak distribution centered at $x = 1/2$ in the low-energy scale to a Dirac delta function centered at $x = 0$ in the high-energy scale, with the aim of investigating whether there are alterations in its modal characteristics during this evolution.

The paper is organized as follows: Sec. II compiles crucial inequalities from Ref. [15] that are relevant to the present study. Sec. III introduces the evolution scheme adopted in this study, namely, the all-orders evolution. Subsequently, Sec. IV presents the results of our analysis, which consists of two parts: examination for non-negativity and continuity, and examination of changes in peak position. Finally, the summary is presented in Sec. V.

II. THE MOMENT PROBLEM

In this section, we briefly introduce the moment problem and present essential inequalities extracted from Ref. [15] that are relevant to the present study. It is important to note that this section adopts a slightly more mathematical approach, and there may be variations in notation compared to other sections. For readers seeking a comprehensive understanding of the moment problem, we recommend consulting references such as Refs. [20, 21].

There exist various types of moment problems, and the specific type of moment problem under consideration can be formulated as follows: Given a sequence of real numbers $(s_k)_{k=0}^m$, it is required to find a non-negative function $f(x)$ that satisfies the equation:

$$s_k = \int_0^1 x^k f(x)\, dx \ (k = 0, 1, 2, \ldots, m)\,. \tag{1}$$

It is worth noting that this problem is not always solvable in general; its resolution requires the given sequence to satisfy certain special conditions. Ref. [15] used not only the non-negativity constraint imposed on $f(x)$ but also other pertinent properties to broaden the scope of the aforementioned problem. Consequently, they obtained the key inequalities essential for the analysis conducted in this study.

Prior to presenting the key inequalities, it is essential to introduce specific terminology and notation. It is termed unimodal if the function $f(x)$ satisfies the following conditions:

$$f(0) = f(1) = 0\,, \tag{2a}$$

$$\exists \lambda \in (0,1), \quad f'(x) \begin{cases} \geq 0, & 0 < x < \lambda \\ \leq 0, & \lambda < x < 1 \end{cases}, \tag{2b}$$

where λ corresponds to the position of the peak. We use $(s_{i+j})_{i,j=0}^n$ to represents the following Hankel matrix:

$$(s_{i+j})_{i,j=0}^n = \begin{pmatrix} s_0 & s_1 & \cdots & s_{n-1} & s_n \\ s_1 & s_2 & \cdots & s_n & s_{n+1} \\ \vdots & \vdots & \ddots & \vdots & \vdots \\ s_{n-1} & s_n & \cdots & s_{2n-2} & s_{2n-1} \\ s_n & s_{n+1} & \cdots & s_{2n-1} & s_{2n} \end{pmatrix}, \tag{3}$$

where i and j, represent the number of rows and columns of the matrix elements, respectively, with values ranging from 0 to n. In addition, we use $A \succ 0$ to indicate that the matrix A is positive definite.

We shall now present the key inequalities relevant to this study. Firstly, the necessary and sufficient condition for the existence of a non-negative continuous function $f(x)$ is that the sequence $(s_k)_{k=0}^m$ satisfies the following condition: for the even case $m = 2n$,

$$(s_{i+j})_{i,j=0}^n \succ 0 \quad \text{and} \quad (s_{i+j+1} - s_{i+j+2})_{i,j=0}^{n-1} \succ 0\,; \tag{4}$$

for the odd case $m = 2n + 1$,

$$(s_{i+j+1})_{i,j=0}^n \succ 0 \quad \text{and} \quad (s_{i+j} - s_{i+j+1})_{i,j=0}^n \succ 0\,. \tag{5}$$

Next, the necessary and sufficient condition for the existence of a non-negative, continuous, and unimodal function $f(x)$ is that the sequence $(s_k)_{k=0}^m$ satisfies the following conditions: for the even case $m = 2n$,

$$\begin{aligned} &\exists \lambda \in (0,1)\,, \quad (\lambda t_{i+j} - t_{i+j+1})_{i,j=0}^n \succ 0 \\ &\text{and} \quad [\lambda t_{i+j+1} - (\lambda+1) t_{i+j+2} + t_{i+j+3}]_{i,j=0}^{n-1} \succ 0\,; \end{aligned} \tag{6}$$

for the odd case $m = 2n + 1$,

$$\begin{aligned} &\exists \lambda \in (0,1)\,, \quad (\lambda t_{i+j+1} - t_{i+j+2})_{i,j=0}^n \succ 0 \\ &\text{and} \quad [\lambda t_{i+j} - (\lambda+1) t_{i+j+1} + t_{i+j+2}]_{i,j=0}^n \succ 0\,, \end{aligned} \tag{7}$$

where $t_k = -k s_{k-1}$.

There are two noteworthy observations regarding these inequalities: First, the conditions imposed on moments are all constituted by the positive definiteness of a specific matrix, whose dimensionality increases with the length of the moment sequence. Consequently, as the length of the moment sequence increases, meeting these conditions becomes progressively more challenging, and simultaneously, the judgement of these conditions can become progressively intricate. Second, these inequalities are only relevant to the existence of $f(x)$, indicating that the sequence $(s_k)_{k=0}^m$ satisfying the respective conditions may correspond to $f(x)$ not possessing the corresponding properties. However the reverse is perfectly clear, i.e., $(s_k)_{k=0}^m$ failing to meet the corresponding condition can not correspond to $f(x)$ exhibiting the specified property.

III. ALL-ORDERS EVOLUTION

In the subsequent section, we present the evolution scheme employed in this paper, namely, the all-orders evolution. The content presented herein is primarily drawn from Section VII of Ref. [9]. The all-orders evolution scheme is based on two foundational assumptions: Firstly, the existence of a hadron scale, denoted as ζ_H, at which the valence quarks carry all the momentum of the hadron, a concept originally introduced in Ref. [5]. Secondly, the existence of a process-independent effective charge in QCD, denoted as $\hat{\alpha}(k^2)$, which remains invariant under renormalization group transformations [9, 22]. For the pion valence quark PDF, the all-orders evolution scheme can be succinctly stated as follows:

$$\frac{\langle x^n\rangle^\zeta}{\langle x^n\rangle^{\zeta_H}} = \exp\left[-\frac{\gamma_0^n}{2\pi}\int_{\zeta_H}^{\zeta}\frac{dy}{y}\hat{\alpha}(y^2)\right], \tag{8}$$

where $\langle x^m\rangle^\zeta$ represents the m-th moment of the pion valence quark PDF at scale ζ ($\zeta_H = 0.331$ GeV), and

$$\gamma_0^n = -\frac{4}{3}\left(3 + \frac{2}{(n+1)(n+2)} - 4\sum_{j=1}^{n+1}\frac{1}{j}\right). \tag{9}$$

Moreover, we use an interpolation of the numerical results [12] as the specific form of $\hat{\alpha}(k^2)$, which is as follows:

$$\hat{\alpha}(k^2) = \frac{\gamma_m \pi}{\ln\left[\frac{\mathcal{K}^2(k^2)}{\Lambda_{\rm QCD}^2}\right]},\ \mathcal{K}^2(y) = \frac{a_0^2 + a_1 y + y^2}{b_0 + y}, \tag{10}$$

where $\gamma_m = 4/\beta_0$, $\beta_0 = 11 - (2/3)n_f$, $n_f = 4$, $\Lambda_{\rm QCD} = 0.234$GeV, with (in GeV^2)

a_0	a_1	b_0
0.104	0.0975	0.121

. (11)

For the sake of simplicity, we refrain from incorporating the corresponding relative errors of the parameters.

To elucidate the properties of $\hat{\alpha}(k^2)$, we compare it with QCD one-loop perturbative running coupling, as depicted in Fig. 1. It is noteworthy that $\hat{\alpha}(k^2)$ remains well defined at all scales without any singularities, and saturates in the infrared region. This property ensures the robust performance of the all-orders evolution scheme over a wide range of scales, which is essential for the investigation of critical phenomena in PDFs. Furthermore, in the ultraviolet region, $\hat{\alpha}(k^2)$ closely matches the QCD one-loop perturbative running coupling. However, a notable deviation between the two becomes apparent around the scale of 0.6 GeV.

IV. NUMERICAL RESULTS

At the outset of our investigation, we need a set of moments as input for the evolution. In this regard, we employ a conventional parametrization of the pion valence quark PDF at the hadron scale ζ_H, formulated as follows [23]:

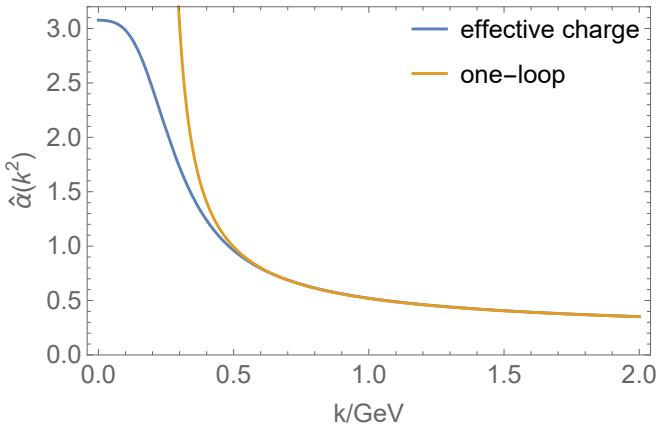

FIG. 1. Comparison between the process-independent effective charge and QCD one-loop perturbative running coupling.

$$u^\pi(x;\zeta_H) = n_\pi \ln[1 + x^2(1-x)^2/\rho^2], \tag{12}$$

where n_π is the normalization constant and $\rho = 0.0660$ is taken from the continuum Schwinger function method (CSM) prediction [24]. Next, we take as input to the evolution the zeroth to eleventh moments of the pion valence quark PDF at the hadron scale given in Table I.

n	0	1	2	3	4	5
$\langle x^n\rangle^{\zeta_H}$	1	0.5	0.29997	0.19995	0.14261	0.10660
n	6	7	8	9	10	11
$\langle x^n\rangle^{\zeta_H}$	0.08248	0.06554	0.05318	0.04390	0.03677	0.03116

TABLE I. The input to the evolution: the zeroth to eleventh moments of the pion valence quark PDF at the hadron scale.

A. Examination for non-negativity and continuity

Given the physical interpretation of the PDF, it is reasonable to anticipate its non-negativity and continuity at $\zeta < \infty$. To verify this conjecture, we conducted an examination of moments at various scales employing the 12 moments enumerated in Table I as input. Our investigation spans the range of scale ζ from ζ_H to 5.2 GeV, with a step size of 1 MeV. Remarkably, we consistently observed the preservation of non-negativity and continuity in the PDF moments over this scale range. This robust outcome is non-trivial and strongly supports to the viability of the all-orders evolution scheme. To further illustrate this point, we artificially float the value of the eleventh-order moment both upwards and downwards to delineate the extent of the 'safe zone' - the region where

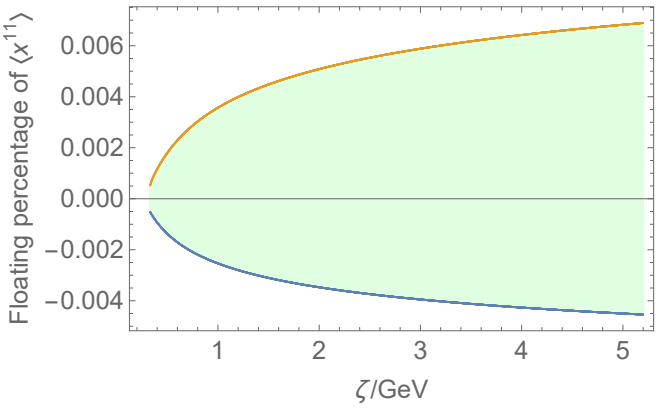

FIG. 2. The green region represents the safe zone of $\langle x^{11}\rangle$, where the non-negativity and continuity of PDF are maintained.

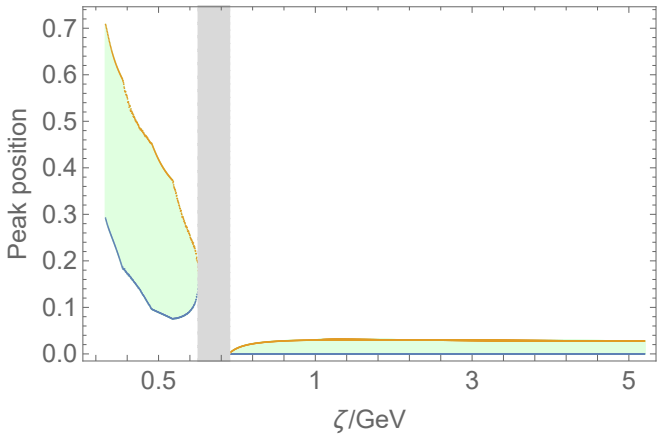

FIG. 3. The green region represents the possible ranges of the peak position of PDF, and the gray region indicates the breakdown of unimodality. Notably, regions that scale less than 1 GeV are enlarged to highlight them.

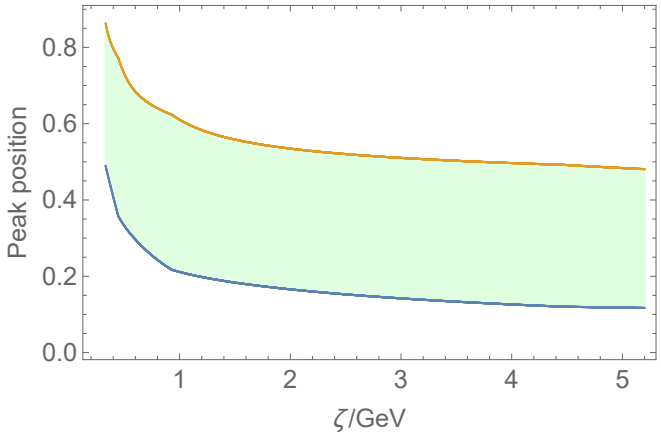

FIG. 4. The green region represents the possible range of the peak position of xPDF.

non-negativity and continuity are both preserved. The result of this analysis is depicted in Fig. 2.

In Fig. 2, it is evident that the safe zone exhibits remarkable narrowness, typically with a width of less than 0.01% of the floating percentage of the eleventh moments. Thus, it is truly remarkable that the all-orders evolution consistently operates within this exceedingly narrow region. Furthermore, the width of the safe region shows a tendency to expand with increasing scale, implying that the moment problem approach is more effective in the low-energy scale region.

B. Examination of changes in peak position

We proceed to analyze the unimodality of the PDF and the transformed one, xPDF. Unlike non-negativity and continuity, discussed previously, unimodality is not necessarily guaranteed. Nevertheless, based on the findings from various methods such as Lattice QCD [18, 19, 25, 26], experimental data [27, 28], global analysis [29, 30], DSE [31, 32], BLFQ-NJL [33], and χCQ [34], it is evident that at 5.2 GeV, the PDF exhibits an approximately unimodal behavior, diverging at $x = 0$, while the xPDF manifests as unimodal with its peak position approximately at $x = 0.3$. Notably, compared to their results at the hadron scale ζ_H, we observe that the peaks of both PDF and xPDF are shifted towards the small x region, a phenomenon that we will delve into further. Employing the aforementioned method, we determined the possible ranges of the positions of the PDF and xPDF peaks, as illustrated in Figs. 3 and 4, respectively.

These two figures provide valuable insights. Firstly, we observe that the results obtained at 5.2 GeV are consistent with the previous discussions, thereby affirming the robustness of our method. Additionally, we observe a notable distinction between the behavior of the PDF and the xPDF regarding the movement of the peak position towards the small x region. The xPDF exhibits a relatively straightforward pattern characterized by a continuous and monotonic variation of the peak range. Consequently, the evolution of the xPDF is naturally anticipated to exhibit a smooth variation. In contrast, the behavior of the PDF is notably more intricate, characterized by a distinct region where the unimodality of the PDF is disrupted. Consequently, the evolution of the PDF is expected to be considerably complex, and we propose that it can be qualitatively characteriszd in three stages. Initially, at low energy scale, before the disruption region, the peak of PDF, originally located at $x = 1/2$, gradually shifts towards the small x region while diminishing in peak magnitude, coinciding with the emergence of a new peak near $x = 0$. Subsequently, within the disrupted region, the height of the new peak gradually converges to that of the old peak, leading to the disruption of unimodality. Ultimately, at high energy scale, beyond the disrupted region, the prominence of the new peak surpasses that of the old peak, thereby reinstating

unimodality.

The bimodal competition process discussed above is highly innovative. Firstly, we note that the corresponding scale at which the unimodal disruption region appears aligns closely with the previously mentioned separation scale between the process-independent effective charge $\hat{\alpha}(k^2)$ and the QCD one-loop perturbative running coupling. In addition, the emergence of the two peaks occurs within distinct domains: one in the nonperturbative (low energy scale) region and the other in the perturbative (high energy scale) region. Therefore, we assert that the competition between the two peaks represents a unique critical phenomenon, wherein the new and old peaks correspond to perturbative and non-perturbative effects, respectively.

V. SUMMARY

In this study, we delve into the intricate domain of hadron physics by employing the moment problem as a pivotal tool to uncover critical phenomena within the foundational pion PDF.

We first introduce essential inequalities associated with the moment problem, which facilitate our understanding of the properties of PDF derived from its moments. Subsequently, we introduce the all-orders evolution scheme, and employ the moments in the form of conventional parameterizations at the hadron scale as inputs for the evolution process. Through this approach, we validate the non-negativity and continuity of the PDF, thereby providing evidence for the validity of the all-orders evolution scheme. Additionally, our finding indicates an enhanced effectiveness of the moment problem in the low energy scale region.

Moreover, our investigation extends to examine the unimodality of the PDF and its corresponding xPDF, thereby elucidating their qualitative evolution patterns. As the scale increases, while the peak position of the xPDF exhibits a gradual shift towards the small-x region, a notable critical phenomenon manifests in the PDF. At the interface of the nonperturbative and perturbative regimes, the PDF exhibits two distinct peaks, illustrating the competing interplay of the nonperturbative and perturbative aspects of QCD dynamics. This profound correspondence enhances our understanding of the intricate relationship between the PDF and the underlying strong interactions.

The method outlined in this paper holds significant potential for broader applicability, and we anticipate extending its scope to encompass other hadrons in future investigations. Furthermore, we believe that validating the correspondence between the two peaks of the PDF and the two effects of QCD - perturbation and non-perturbation - using alternative methods can further strengthen our findings.

ACKNOWLEDGMENTS

Work supported by National Natural Science Foundation of China (grant no. 12135007). MD is grateful for support by Helmholtz-Zentrum Dresden-Rossendorf High Potential Programme.

[1] R. P. Feynman, Phys. Rev. Lett. **23**, 1415 (1969).
[2] J. D. Bjorken, Phys. Rev. **179**, 1547 (1969).
[3] J. C. Collins, D. E. Soper, and G. F. Sterman, Adv. Ser. Direct. High Energy Phys. **5**, 1 (1989), arXiv:hep-ph/0409313.
[4] G. Altarelli, Phys. Rept. **81**, 1 (1982).
[5] R. L. Jaffe and G. G. Ross, Phys. Lett. B **93**, 313 (1980).
[6] M. Diehl and P. Stienemeier, Eur. Phys. J. Plus **135**, 211 (2020), arXiv:1904.10722 [hep-ph].
[7] L. Chang and A. W. Thomas, Phys. Lett. B **749**, 547 (2015), arXiv:1410.8250 [nucl-th].
[8] M. Ding, K. Raya, D. Binosi, L. Chang, C. D. Roberts, and S. M. Schmidt, Chin. Phys. C **44**, 031002 (2020), arXiv:1912.07529 [hep-ph].
[9] K. Raya, Z.-F. Cui, L. Chang, J.-M. Morgado, C. D. Roberts, and J. Rodriguez-Quintero, Chin. Phys. C **46**, 013105 (2022), arXiv:2109.11686 [hep-ph].
[10] P.-L. Yin, Y.-Z. Xu, Z.-F. Cui, C. D. Roberts, and J. Rodríguez-Quintero, Chin. Phys. Lett. **40**, 091201 (2023), arXiv:2306.03274 [hep-ph].
[11] G. Altarelli and G. Parisi, Nucl. Phys. B **126**, 298 (1977).
[12] Z.-F. Cui, J.-L. Zhang, D. Binosi, F. de Soto, C. Mezrag, J. Papavassiliou, C. D. Roberts, J. Rodríguez-Quintero, J. Segovia, and S. Zafeiropoulos, Chin. Phys. C **44**, 083102 (2020), arXiv:1912.08232 [hep-ph].
[13] Y. Lu, L. Chang, K. Raya, C. D. Roberts, and J. Rodríguez-Quintero, Phys. Lett. B **830**, 137130 (2022), arXiv:2203.00753 [hep-ph].
[14] Y. Yu, P. Cheng, H.-Y. Xing, F. Gao, and C. D. Roberts, Contact interaction study of proton parton distributions (2024), arXiv:2402.06095 [hep-ph].
[15] X. Wang, M. Ding, and L. Chang, Sieving parton distribution function moments via the moment problem (2023), arXiv:2308.14871 [hep-ph].
[16] L. Chang, I. C. Cloet, J. J. Cobos-Martinez, C. D. Roberts, S. M. Schmidt, and P. C. Tandy, Phys. Rev. Lett. **110**, 132001 (2013), arXiv:1301.0324 [nucl-th].
[17] C. Alexandrou, S. Bacchio, I. Cloet, M. Constantinou, K. Hadjiyiannakou, G. Koutsou, and C. Lauer (ETM), Phys. Rev. D **103**, 014508 (2021), arXiv:2010.03495 [hep-lat].
[18] C. Alexandrou, S. Bacchio, I. Cloët, M. Constantinou, K. Hadjiyiannakou, G. Koutsou, and C. Lauer (ETM), Phys. Rev. D **104**, 054504 (2021), arXiv:2104.02247 [hep-lat].
[19] B. Joó, J. Karpie, K. Orginos, A. V. Radyushkin, D. G. Richards, R. S. Sufian, and S. Zafeiropoulos, Phys. Rev. D **100**, 114512 (2019), arXiv:1909.08517 [hep-lat].
[20] K. Schmüdgen, Ten lectures on the moment problem (2020), arXiv:2008.12698 [math.FA].

[21] K. Schmüdgen, *The Moment Problem* (Springer, Leipzig, 2017).

[22] G. Grunberg, Phys. Rev. D **29**, 2315 (1984).

[23] Z. F. Cui, M. Ding, J. M. Morgado, K. Raya, D. Binosi, L. Chang, F. De Soto, C. D. Roberts, J. Rodríguez-Quintero, and S. M. Schmidt, Phys. Rev. D **105**, L091502 (2022), arXiv:2201.00884 [hep-ph].

[24] Y. Lu, Y.-Z. Xu, K. Raya, C. D. Roberts, and J. Rodríguez-Quintero, Pion distribution functions from low-order mellin moments (2023), arXiv:2311.08565 [hep-ph].

[25] R. S. Sufian, J. Karpie, C. Egerer, K. Orginos, J.-W. Qiu, and D. G. Richards, Phys. Rev. D **99**, 074507 (2019), arXiv:1901.03921 [hep-lat].

[26] R. S. Sufian, C. Egerer, J. Karpie, R. G. Edwards, B. Joó, Y.-Q. Ma, K. Orginos, J.-W. Qiu, and D. G. Richards, Phys. Rev. D **102**, 054508 (2020), arXiv:2001.04960 [hep-lat].

[27] J. S. Conway *et al.*, Phys. Rev. D **39**, 92 (1989).

[28] M. Aicher, A. Schafer, and W. Vogelsang, Phys. Rev. Lett. **105**, 252003 (2010), arXiv:1009.2481 [hep-ph].

[29] P. C. Barry, N. Sato, W. Melnitchouk, and C.-R. Ji, Phys. Rev. Lett. **121**, 152001 (2018), arXiv:1804.01965 [hep-ph].

[30] N. Y. Cao, P. C. Barry, N. Sato, and W. Melnitchouk (Jefferson Lab Angular Momentum), Phys. Rev. D **103**, 114014 (2021), arXiv:2103.02159 [hep-ph].

[31] C. Chen, L. Chang, C. D. Roberts, S. Wan, and H.-S. Zong, Phys. Rev. D **93**, 074021 (2016), arXiv:1602.01502 [nucl-th].

[32] K. D. Bednar, I. C. Cloët, and P. C. Tandy, Phys. Rev. Lett. **124**, 042002 (2020), arXiv:1811.12310 [nucl-th].

[33] J. Lan, C. Mondal, S. Jia, X. Zhao, and J. P. Vary, Phys. Rev. D **101**, 034024 (2020), arXiv:1907.01509 [nucl-th].

[34] A. Watanabe, T. Sawada, and C. W. Kao, Phys. Rev. D **97**, 074015 (2018), arXiv:1710.09529 [hep-ph].